Simulation of FT-IR and FT-Raman Spectra Based on Scaled DFT Calculations, Vibrational Assignments, Hyperpolarizability, NMR Chemical Shifts and Homo-Lumo Analysis of 1-Chloro-4-Nitrobenzene

S.Seshadri [1] , Rasheed .M.P [2]

[1](Associate Professor and Head, PG and Research Department of Physics, Urumudhanalakshmi College, Trichy-19)
[2] (Research Scholar, PG and Research Department of Physics, Urumudhanalakshmi College , Trichy-19)
Corresponding Author: Rasheed M P   Mob 9947234807

Abstract: This work deals with the vibrational spectroscopy of 1-chloro-4-nitrobenzene (1C4NB) by means of quantum chemical calculations. The solid phase FT-IR and FT-Raman spectra of 1-chloro-4-nitrobenzene (1C4NB) have been recorded in the regions 4000–400 and 3500-50 cm^{-1} respectively. The fundamental vibrational frequencies and intensities of vibrational bands were evaluated using density functional theory (DFT) with the standard B3LYP/6-311+G(d.p) method and frequencies were scaled using various scale factors. Simulation of infrared and Raman spectra utilizing the results of these calculations led to excellent overall agreement with the observed spectral patterns. The SQM approach applying selective scaling of the DFT force field was shown to be superior to the uniform scaling method in its ability to allow for making modifications in the band assignment, resulting in more accurate simulation of FT-IR and FT-Raman Spectra. The ^1H and ^{13}C nuclear magnetic resonance chemical shifts of the molecule were also calculated using the gauge independent atomic orbital (GIAO) method. The theoretical and experimental UV–VIS spectra of 1-chloro-4-nitrobenzene (1C4NB) were recorded and compared and the electronic properties, such as HOMO (Highest Occupied Molecular Orbital) and LUMO (Lowest Unoccupied Molecular Orbital) energies were performed by time-dependent DFT (TD-DFT) approach. Information about the size, shape and charge density distribution and site of chemical reactivity of the molecule has been obtained by mapping electron density isosurface with Molecular Electro Static Potential (MESP).The dipole moment , polarizability, first order hyperpolarizability and mullikkan atomic charges of the title molecule were computed using DFT calculations. In addition Chemical reactivity and thermodynamic properties of 1C4NB at different temperatures were also computed.
Key words: DFT, FTIR, FT-Raman, NMR, UV-Vis, HOMOLUMO, Hyperpolarizability, 1C4NB

I.   INTRODUCTION

1-chloro-4-nitrobenzene (1C4NB) is an organic compound with the formula $C_6H_4ClNO_2$. It is a pale yellow crystalline solid at room temperature with a sweet odour and is slightly soluble in water (243 mg/L at 20^0C). Its physical properties are given below. Chemical Class: nitro aromatic, Molecular mass: 157.56 g/mol, Boiling Point: 242^0C,   Melting Point: 82.6^0C, Vapour Pressure: 0.2 mm Hg (at 30^0C).

It is a common intermediate in the production of a number of industrially useful compounds. 1C4NB is used in the chemical industry. It is used in the synthesis of industrial chemicals like paranitrophenol, paranitroaniline, paraaminophenol, 4-nitroanisole, and para-anisidine. It is used in the preparation of pesticides like parathion, methyl parathion, ethyl parathion and nitrophen. It is widely used in the drug industry, in the synthesis of analgesic drugs like phenacetin and acetaminophen, and the antimicrobial drug like dapsone, which is used to treat leprosy among other conditions [1]. 1C4NB is also used in the synthesis of 4-nitrodiphenylamine based antioxidants for rubber. It is prepared industrially by nitration of chlorobenzene [2].

International Journal for Research in Applied Science & Engineering Technology (IJRASET)

II.   EXPERIMENTAL DETAILS

Spectroscopically pure polycrystalline sample of 1C4NB was obtained from the Lancaster chemical company, UK, and used as such for the spectral measurements. The room temperature Fourier transform infrared spectra of the 1C4NB compound was measured with KBr and poly ethylene pellets technique in the 4000–400 cm^{-1} regions at a resolution of ±1 cm^{-1} using Perkin-Elmer Spectrum RX1 spectro photometer equipped with He-Ne laser source.

The FT-Raman spectra of 1C4NB was recorded on a BRUKER IFS-66V model interferometer equipped with an FRA-106 FT-Raman accessory in the 3500–50 cm^{-1} stokes region using the 1064 nm line of a Nd:YAG laser for excitation operating at 200mW power. The reported wave numbers are believed to be accurate within ±1 cm^{-1}.

III.   COMPUTATIONAL DETAILS

The molecular geometry optimization, energy and vibrational frequency calculations were carried out for 1C4NB with Gaussian 09 software package [3] using the Beeke-3-Lee-Yang-Parr (B3LYP) functional[4,5] supplemented with the standard 6-311+G(d,p) basis set. The Cartesian representation of the theoretical force constants have been computed at optimized geometry having C$_1$ point group symmetry. Scaling of the force field was performed according to the SQM procedure [6,7] using selective scaling in the natural internal coordinate representation [8,9]. Transformation of the force field and subsequent normal coordinate analysis including the least square refinement of the scaling factors, calculation of the potential energy distribution (PED) and the prediction of IR and Raman intensities were done on a PC with the MOLVIB program written by Sundius [10,11]. For the plots of simulated IR and Raman spectra, pure Lorentzian band shapes were used with a bandwidth (FullWidthHalfMaximum,FWHM) of 10 cm^{-1}. The symmetry of the molecule was also helpful in making vibrational assignments. The symmetries of the vibrational modes were determined by using the standard procedure [12] of decomposing the traces of the symmetry operation into the irreducible representation. The symmetry analysis for the vibrational modes of 1C4NB was presented in some details in order to describe the basis for the assignments. By combining the results of the Gauss view program [13] with symmetry considerations, vibrational frequency assignments were made with a high degree of confidence. There is always some ambiguity in defining internal coordinates. However, the defined coordinate form complete set and matches quite well with the motions observed using the Gaussview 5 program.

IV.   PREDICTION OF RAMAN INTENSITIES

The computational prediction of vibrational spectra is among the important areas of application for modern quantum chemical methods because it allows the interpretation of experimental spectra and can be very instrumental for the identification of unknown species. A vibrational spectrum consists of two characteristics, the frequency of the incident light at which the absorption occurs and how much of the radiation is absorbed. The first quantity can be obtained computationally by calculating the harmonic vibrational frequencies of a molecule.

In the case of an infrared spectrum, the intensity is related to the square of the infinitesimal change of the electric dipole moment with respect to the normal coordinates. But the intensities of Raman scattering depend on the square of the infinitesimal change of the polarizability with respect to the normal coordinates. The prediction of Raman intensities was carried out by following the procedure outlined below. The Raman activities (*Si*) calculated by the Gaussian 09 program and adjusted during scaling procedure with MOLVIB were converted to relative Raman intensities (*Ii*) using the following relationship derived from the basic theory of Raman scattering [14-16].

$$I_i = \frac{f\,(\nu_o - \nu_i)^4 S_i}{\nu_i \left[1 - \exp\left(\dfrac{-hc\,\nu_i}{kT}\right)\right]}$$

where ν_0 is the exciting frequency (in cm^{-1} units), ν_i the vibrational wave number of the ith normal mode, h, c and k the universal constants, and f is the suitably chosen common normalization factor for all the peak intensities. Calculated Raman intensities and Raman activities were reported in TABLE III.

International Journal for Research in Applied Science & Engineering Technology (IJRASET)

V.   RESULTS AND DISCUSSION
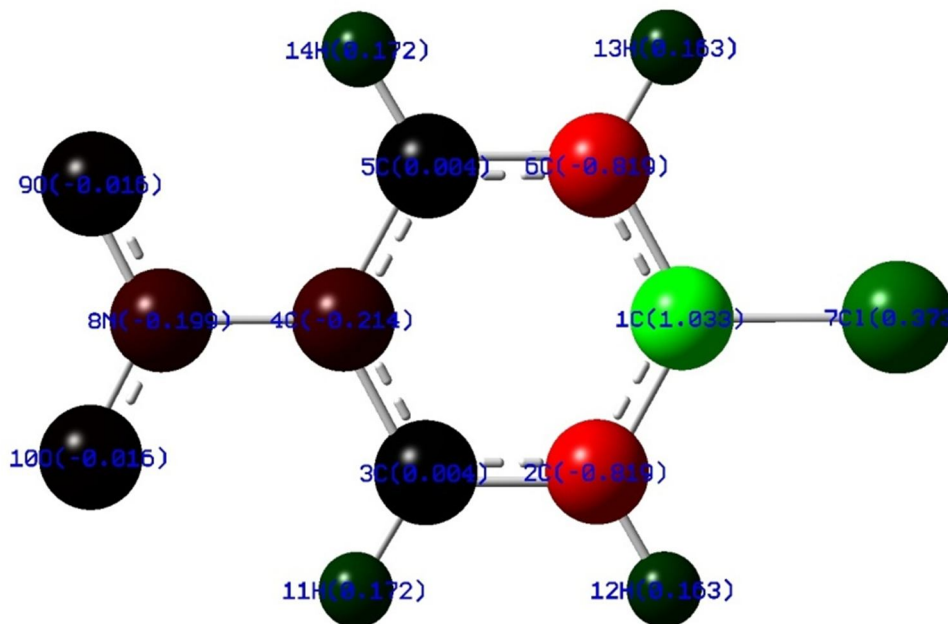
A.   Molecular geometry

Fig. 1. Optimized Molecular Structure of 1C4NB with atom numbering scheme and mullikkan atomic charges

The molecular structure along with numbering of atoms of 1C4NB was as shown in the Fig.1 . The Global minimum energies of 1-chloro-4-nitrobenzene calculated by Density Functional Theory structure optimization for different basis sets such as B3LYP/6-31+ G(d,p) ,B3LYP/6-31++ G(d,p) , B3LYP/6-311+ G(d,p) and B3LYP/6-311++ G(d,p) are given in Table 1

TABLE 1-
GLOBAL MINIMUM ENERGY OF 1-CHLORO-4-NITROBENZENE OBTAINED BY DFT STRUCTURE OPTIMIZATION

Method (B3LYP)	Energies (Hartees)
6-31 + G(d,p)	-896.4453805
6-31 + +G(d,p)	-896.4455305
6-311 + G(d,p)	-896.4958349
6-311 + +G(d,p)	-896.4961254

Geometry optimization is the procedure that attempts to find the configuration of minimum energy of the molecule. The procedure calculates the wave function and the energy at a starting geometry and then proceeds to search a new geometry of a lower energy. This is repeated until the lowest energy geometry is found. The procedure calculates the force on each atom by evaluating the gradient or the first derivative of the energy with respect to atomic positions. Sophisticated algorithms are then used at each step to select a new geometry, aiming for rapid convergence to the geometry of the lowest energy. In the final, minimum energy geometry the force on each atom is zero.

The optimized geometric parameters like bond length, bond angles and dihedral angles of 1-chloro-4-nitrobenzene (1C4NB) were calculated and given in Table II .The C-C bond lengths in the benzene ring obtained from B3LYP/6-311+G(d,p) ranges from 1.389488 to 1.394212 Å and C-H bond length ranges from 1.08122 to 1.082014 Å.

International Journal for Research in Applied Science & Engineering Technology (IJRASET)

TABLE II

THE OPTIMIZED GEOMETRICAL PARAMETERS (BOND LENGTH, BOND ANGLES AND DIHEDRAL ANGLES) OF
1-CHLORO-4-NITROBENZENE OBTAINED BY B3LYP/6-311+G(D,P) BASIS SET

Bond Length	Angstrom	Bond Angles	Degree	Dihedral Angles	Degree
C2-H12	1.082012	C1-C2-C3	119.28	H12-C2-C1-C6	-179.98
C3-H11	1.08123	H12-C2-C1	120.16	H11-C3-C4-N8	-0.01
C5-H14	1.08122	H11-C3-C2	121.26	H14-C5-C6-C1	-180
C6-H13	1.082014	H14-C5-C6	121.26	H13-C6-C1-C2	-180
O9-N8	1.224518	H13-C6-C5	120.56	O9-N8-C4-C3	-180
O10-N8	1.224503	O9-N8-C4	117.61	C6-C5-C4-C3	-0.01
C3-C2	1.389518	O10-N8-O9	124.79	C1-C2-C3-C4	0
C6-C5	1.389488	C6-C5-C4	118.99	C5-C4-C3-C2	0
C1-C2	1.394212	C4-C3-C2	118.99	O10-C4-O9-N8	0
C4-C3	1.391269	C5-C4-C3	121.98	Cl7-C2-C6-C1	0.01
C5-C4	1.391297	N8-C4-C5	119.01	N8-C3-C5-C4	0
N8-C4	1.477472	Cl7-C1-C6	119.26		
Cl7-C1	1.749541				

B. Vibrational assignments

Vibrational spectroscopy has been shown to be effective in the identification of functional groups of organic compounds as well as in studies on molecular conformations and reaction kinetics [17]

The symmetry possessed by the title molecule helps to determine and classify the actual number of fundamental vibrations of the system. The observed spectrum is explained on the basis of C_1 point group symmetry. The title molecule consists of 14 atoms, which undergo 36 normal modes of vibrations .The total number of 36 fundamental vibrations (3N-6, where N is the number of atoms) are distributed as

Γ_{vib} = 25 A' (In plane vibrations;2N-3) + 11 A"(out of plane vibrations;N-3)

All vibrations are active both in Raman and infrared absorption. The detailed vibrational assignment of fundamental modes of 1C4NB along with the calculated IR and Raman frequencies, IR intensities, Raman activities ,Raman intensities and normal mode descriptions using PED (Potential Energy Distribution) are reported in Table III. The calculated frequencies are usually higher than the corresponding experimental quantities, due to the combination of electron correlation effects and basis set deficiencies.
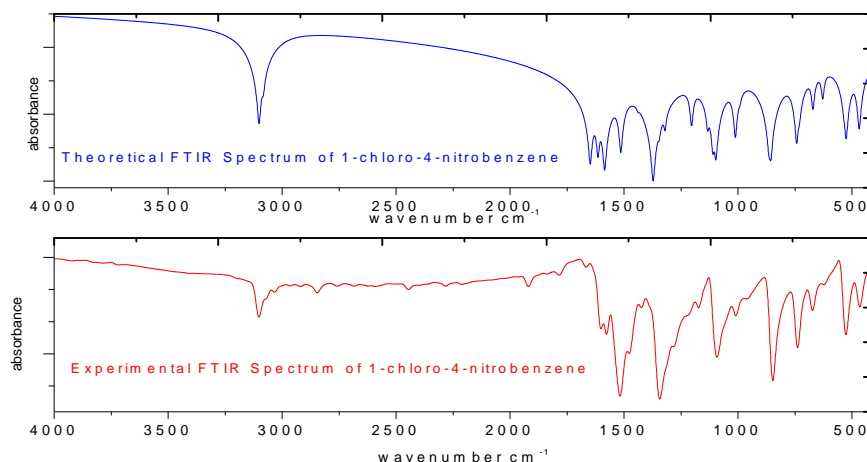

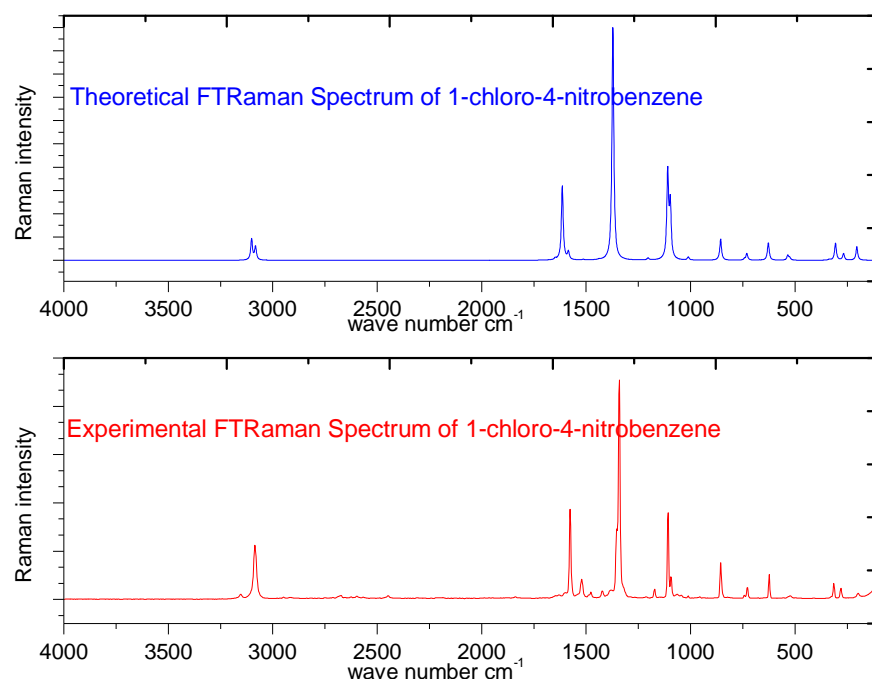Fig. 2 The observed and simulated FT-IR spectra of the 1C4NB

635

Fig. 3 The observed and simulated FT-Raman spectra of the 1C4NB

For visual comparison, the observed and simulated FT-Raman and FT-IR spectra of the 1C4NB were produced in common frequency scales in Figs. 2 and 3 respectively. The root mean square error between unscaled (B3LYP/6-311+G(d,p)) and experimental frequencies is found to be 69.8 cm^{-1}. In order to reproduce the observed frequencies, refinement of scaling factors are applied and optimized via least square refinement algorithm which resulted in a weighted RMS deviation of about 7.9 cm^{-1} between the experimental and scaled frequencies. After applying the scaling factors, the theoretical calculations reproduce the experimental data well in agreement.

1) *Potential Energy Distribution:* To check whether the chosen full set of assignments contributes the maximum to the potential energy associated with normal coordinates of the molecules, the potential energy distribution (PED) was calculated using the relation

$$PED = (F_{ii} L_{ik}^{2})/ \lambda_{k}$$

where F_{ii} are the force constants defined by the damped least square technique, L_{ik} the normalised amplitude of the associated element (i,k) and λ_{k} the Eigen value corresponding to the vibrational frequency of the element k. The PED contributions corresponding to each of the observed frequencies over 10% are only listed in the present work (Table III).

2) *C–H vibrations:* The presence of C-H stretching vibrations in the region 3000 - 3200 is common for heteroaromatic structure. In the present study the C-H stretching vibrations of the title compound are observed at 3101.4 and 3063.5 cm^{-1} in the FT-IR spectrum and 3085.6 cm^{-1} in the FT-Raman spectrum. The calculated wave numbers at 3251.2, 3232.1 and 3219.6 cm^{-1} by B3LYP/6-311+G(d,p) method are assigned to C-H stretching vibrations and are scaled to 3101.4, 3100.0 and 3083.1 cm^{-1} respectively. The C-H out of plane bending vibrations are occurring in the region 900-667 cm^{-1} [18].In the present investigation the computed wave numbers at 896.4,837.7 and 779.6 cm^{-1} by B3LYP/6-311+G(d,p) method are assigned to C-H out of plane vibrations and the scaled values are in good agreement with the experimental values. The assignments of other in-plane and out-of-plane C-H bending vibrations are as shown in Table III.

3) *C-CI vibrations:* The assignments of C–CI stretching and deformation vibration have been made by comparison with halogen substituted benzene derivatives [19-23] assigned vibrations of the C–X group (X = CI,I, Br) in the frequency range of 1129–480 cm^{-1}. Based on the above literature data, the theoretically computed by B3LYP/6-311+G(d,p) method at 972.9 , 619 and 382.8 cm^{-1} are assigned to C–Cl stretching vibrations show good agreement with experimental FTIR and FTRaman bands. The in

636

plane bending vibrations of C-Cl observed at 198.1 cm^{-1} in FT-Raman spectrum. The calculated wavenumbers for C-Cl in plane bending vibrations are at 299.1 and 149.1 cm^{-1} computed by B3LYP/6-311+G(d,p) method and they are scaled to 325.4 and 195.7 cm^{-1} respectively.The C–Cl out of plane bending vibrations computed by B3LYP/6-311+G(d,p) at 543.5 and 363.7 cm^{-1} and the scaled values are in good agreement with the recorded spectrum

4) *C-N Vibrations:* The mixing of several bands are possible in this region. The C-N stretching frequency is a rather difficult task. In the present study the band observed at 1666.2 cm^{-1} in FT-IR spectrum is attributed to C-N bending vibration. The theoretically calculated value of corresponding C-N bending vibration is predicted at 1629.6 cm^{-1} and it is scaled to 1665.5 cm^{-1}.This bending vibration is mixed with C-C and N-O stretching vibrations. The bands observed at 1333,1065 and 770.8 cm^{-1} are assigned to C-N stretching vibrations. These modes are also mixed with other vibrations like C-C and N-O stretching vibrations and C-N-O,C-C-H and Ring bending vibrations.

5) *Ring vibrations:* There are six equivalent C-C bonds in benzene and consequently there will be six C-C stretching vibrations. In addition, there are several C-C-C in-plane and out-of-plane bending vibrations of the ring carbons. However, due to high symmetry of benzene, many modes of vibrations are infrared inactive. In general, the bands around 1400 to 1650 cm^{-1} in benzene derivatives are assigned to skeletal stretching C-C bands[24]. In the case of title compound the carbon stretching vibrations have been observed at 1666.2 ,1601.3, 1576.3, 1517.4, 1423.9 and 1343.4 cm^{-1} in the FT-IR spectrum and 1576.7,1521.36,1422.78 and 1341.44 cm^{-1} in FT-Raman spectrum were assigned to C-C stretching vibration which show good agreement with scaled frequencies. The measured wavenumbers at 1629.6, 1606.7, 1499.6, 1423.7,1397.8 and 1276.8 cm^{-1} by B3LYP method are assigned to C-C stretching vibrations and they are scaled to 1665.5,1595,1585.1,1516.2,1423.2 and 1346.6 cm^{-1} respectively. It is clear from the above values that the difference between observed and scaled frequencies is very small. In general, the C–C–C out-of-plane and in-plane-bending vibrational wavenumber observed in FTIR spectrum and FT-Raman spectrum shows good agreement with theoretically computed wavenumber.

6) *Nitro group vibrations:* Nitro group compounds are characterized by two bands; a very strong asymmetric stretch at 1540 1614 cm^{-1} and a strong symmetric stretch at 1320–1390cm^{-1} [25]. For our title compound 1C4NB, the strong IR band identified at 1576.3 cm^{-1} and another strong band at1576.7 in FT Raman spectrum and 1333 cm^{-1} in B3LYP method were described to NO$_2$ stretching vibration. This is in consistent with PED as shown in Table III . More recent work however has emphasized that for Raman scattering from totally symmetric molecular vibrations the intensity is governed to a large extent by the Franck Condon (FC) principle and these in turn are related to the displacement of the molecular geometry along the normal coordinates in the excited electronic state [26]. This fact tends to limit the origin of vibrational Raman intensity to low lying electronic states. Indeed in the higher electronic state the change in the electronic bonding of the molecule may be so great that the normal mode structure in these higher electronic states is completely different from the lowest excited state or the ground state. Instead of preserving the Raman intensity in a single vibration it is spread over all 3N-6 vibrations so that the measured resonance Raman intensity in any one band is negligible. This may be the origin of the recent observation that resonance with higher electronic excited states gives much weaker resonance enhancement than that obtained with lower lying excited states [27]. It may be that for certain molecular vibrations, the lowest lying allowed excited electronic state may be the maximum. In order to explain these results they use the theory, in which it is assumed that in the observation of equal excited state displacements for the symmetric nitrogen–oxygen stretching vibrations has an interesting corollary. The origin of this displacement almost certainly resides in the involvement of the electrons in the N–O bonds in the **π** to **π*** electronic transition of the lowest excited state. This involvement causes a change (probably a reduction) in the bond order of the N-O bonds, resulting in a change in the N-O bond lengths in going from the ground to the excited electronic state. It seems that in each of these compounds this change in bond order is the same so that the involvement of the N–O bonding electrons in the **π** to **π*** transition remains constant for this series of chemically related compounds. For 1C4NB the N-O bond length is of the same order as that of nitrophenol [28]. Aromatic nitro compound have a band of weak to medium intensity in the region 590–500 cm^{-1} [29] due to the in plane deformation mode of NO$_2$ group. The deformation vibrations of NO$_2$ (rocking, wagging, scissoring and twisting) contribute to several modes in the low frequency region [30]. The band observed at 738.4 cm^{-1} and 465.5 cm^{-1} in IR spectrum and band at 280.6 cm^{-1} in FT Raman spectrum of 1C4NB with a PED contribution of 55%, 14% and 27% respectively are assigned to NO$_2$ rocking, wagging and scissoring modes. Based on the SQM results the NO$_2$ torsional mode can be expected to appear below 100 cm^{-1} only. The experimental counter part of this mode is possible only in far IR spectra. Our SQM calculated frequency 51.3 cm^{-1} agrees well with experimental FT Raman band at 60 cm^{-1}.

International Journal for Research in Applied Science & Engineering Technology (IJRASET)

TABLE III

OBSERVED AND B3LYP/6-311+G(D,P) LEVEL CALCULATED VIBRATIONAL FREQUENCIES (IN CM^{-1}) OF 1C4NB

No	symmetry species	Observed frequency		Calculated frequency (cm^{-1}) with B3LYP/6-311++G(d,p) force field					Characterisation of normal modes with PED%
		IR (cm^{-1})	Raman (cm^{-1})	Unscaled (cm^{-1})	Scaled (cm^{-1})	IR intensity	Raman activity Si	Raman intensity (Ii)	
1	A'	3101.	-	3251.2	3101.	4.322	174.76	302.98	υCH (99)
2	A'	-	3085.6	3232.1	3100.	2.665	10.954	19.54	υCH (99)
3	A'	3063.	-	3219.6	3083.	0.537	62.871	111.25	υCH (99)
4	A'	-	-	1663.1	1682.	0.019	52.349	92.74	υCH (99)
5	A'	1666.	-	1629.6	1665.	257.85	12.973	16.16	υCC (38),υ NO (28), bCNO(
6	A'	1601.	-	1606.7	1595	53.842	132.72	1820.7	υCC (67), bCH (22)
7	A'	1576.	1576.7	1499.6	1585.	28.021	5.64	220.59	υNO (60), υCC (27)
8	A'	1517.	1521.3	1423.7	1516.	57.835	0.269	25.98	bCH (64), υCC (32)
9	A'	1423.	1422.7	1397.8	1423.	4.649	0.394	10.26	υ CC (49), bCH (39)
10	A'	-	-	1333	1411.	355.23	343.63	10.259	υNO (72), υCN (15),
11	A'	1343.	1341.4	1276.8	1346.	1.354	0.224	0	υCC (56), bCH (35)
12	A'	-	-	1179.5	1298.	12.589	0.091	8.78	υCC (64), bCH (33)
13	A'	-	-	1152.3	1204.	11.686	4.358	41.38	bCH (73), υCC (24)
14	A'	-	-	1121.3	1127.	5.765	0.284	10.24	bCH (63), υCC (32)
15	A'	-	1108.1	1065	1106.	4.358	36.547	2653	CC (37), υCN(32), bCH (16),
16	A'	-	1093.7	972.9	1090.	138.83	112.57	1463.0	υCC (54), υCCl (27), bCH
17	A'	-	1011.8	910.3	1012.	15.359	1.996	62.55	bRing (69), υCC (19)
18	A"	1010.	-	896.4	1006.	0.001	0.002	0.1	gCH (92), tRing (7)
19	A"	-	-	837.7	992.1	0.599	0.049	1.91	gCH (81), tRing (15)
20	A"		857	779.6	863.8	48.706	0.479	939.83	gCH (72), tRing (11)
21	A'	-	-	770.8	856.3	73.565	15.511	25.5	bCNO(46),υCN(16), bRing(13),
22	A"	846.8	-	698.1	844.1	0.001	0.027	1.61	gCH (99)
23	A"	738.4	-	673.5	737.1	26.794	0.731	291.71	tNO2(55), gCN(16), gCH(14),
24	A'	-	728.4	619	735.4	2.116	5.216	56.42	bRing (48), υCCl(21), bCNO(11)
25	A"	673.2	-	543.5	671.4	2.219	0.113	18.43	tRing (69), gCl (14)
26	A'	-	623.9	501.5	627	0.803	7.258	774.67	bRing (80)
27	A'	-	523.3	435.5	532.3	17.999	0.94	416.82	bCNO(74), bCN(12)
28	A'	526.3	-	382.8	527.8	1.062	2.213	118.85	υCCl(44), CN(30), bRing(13)
29	A"	465.5	-	363.7	468.2	9.594	0.003	0.21	tRing(43),gCN(21), gCl(19),
30	A"	-	-	328	413.4	0	0.001	0.05	tRing(78), gCH(16)
31	A'	-	-	299.1	325.4	0.016	0.095	21.9	bCCl(41), bCNO(33), bCN(13),
32	A'	-	314.8	219	309	0.29	2.703	1353.2	bRing(44), υCN(23), υCCl(19)
33	A"	-	280.6	178.7	270.3	1.145	0.807	528.31	gCN(39), tNO2(27), gCl(18),
34	A'	-	198.1	149.1	195.7	3.187	1.048	1316.7	bCN(36), bCCl(36), bCNO(20)
35	A"	-	-	92.5	90.9	3.393	0.029	222.44	tRing (47),gCH(19), gCN(16),
36	A"	-	60	51.3	51	0.001	0.007	143.54	tNO2 (100)

Abbreviations used: υ .Stretching vibrations; b. in plane bending; g. out of plane deformation;
t. torsion; bRing. Bending ring vibration; tRing. Torsional ring vibration

638

International Journal for Research in Applied Science & Engineering Technology (IJRASET)

PED more than 10 % only are given

C. Nonlinear optical (NLO) effects

The NLO activity provide the key functions for frequency shifting, optical modulation, optical switching and optical logic for the developing technologies in areas such as communication, signal processing and optical interconnections [31]. The first static hyperpolarizability (β_{tot}) and its related properties (β, α_o and $\Delta\alpha$) have been calculated using B3LYP/6-31G(d,p) level based on finite field approach. In the presence of an applied electric field, the energy of a system is a function of the electric field and the first hyperpolarizability is a third rank tensor that can be described by a 3×3×3 matrix. The 27 components of the 3D matrix can be reduced to 10 components because of the Kleinman symmetry [32]. The matrix can be given in the lower tetrahedral format. It is obvious that the lower part of the 3×3×3 matrices is a tetrahedral. The components of β are defined as the coefficients in the Taylor series expansion of the energy in the external electric field. When the external electric field is weak and homogeneous, this expansion is given below:

$$E = E_0 - \mu_\alpha \ F_\alpha - \tfrac{1}{2}\ \alpha_{\alpha\beta}\ F_\alpha\ F_\beta - \tfrac{1}{6}\ \beta_{\alpha\beta\gamma}\ F_\alpha\ F_\beta\ F_\gamma + \ldots\ldots\ldots$$

Where E_o is the energy of the unperturbed molecules, F_α is the field at the origin, μ_α ,$\alpha_{\alpha\beta}$ and $\beta_{\alpha\beta\gamma}$ are the components of dipole moment, polarizability and first hyperpolarizability, respectively.

The total static dipole moment μ_{tot}, the mean polarizability α_o, the anisotropy of the polarizability $\Delta\alpha$ and the mean first hyperpolarizability β_{tot}, using the x, y and z components are defined as:

Total static dipole moment ($\boldsymbol{\mu_{tot}}$)

$$\mu_{tot} = (\mu_x^2 + \mu_y^2 + \mu_z^2)^{\frac{1}{2}}$$

The mean polarizability ($\boldsymbol{\alpha_o}$)

$$\alpha_0 = \frac{1}{3}(\alpha_{xx} + \alpha_{yy} + \alpha_{zz})$$

The anisotropy of the polarizability ($\Delta\boldsymbol{\alpha}$)

$$\Delta\alpha = \frac{1}{\sqrt{2}}\sqrt{\left[\left(\alpha_{xx} - \alpha_{yy}\right)^2 + \left(\alpha_{yy} - \alpha_{zz}\right)^2 + (\alpha_{zz} - \alpha_{xx})^2 + 6\alpha_{xz}^2\right]}$$

Components of first hyperpolarizability can be calculated by using the expression

$$\beta_i = \beta_{iii} + \sum_{i \neq j}\left[\frac{(\beta_{ijj} + 2\beta_{jii})}{3}\right]$$

Using x, y, z components the magnitude of first hyperpolarizability ($\boldsymbol{\beta_{tot}}$) can be calculated as

$$\beta_{tot} = \sqrt{(\beta_x^2 + \beta_y^2 + \beta_z^2)}$$

Where $\boldsymbol{\beta_x}$, $\boldsymbol{\beta_y}$ and $\boldsymbol{\beta_z}$ are

$$\beta_x = (\beta_{xxx} + \beta_{xyy} + \beta_{xzz})$$
$$\beta_y = (\beta_{yyy} + \beta_{yzz} + \beta_{yxx})$$
$$\beta_z = (\beta_{zzz} + \beta_{zxx} + \beta_{zyy})$$

$$\beta_{tot} = \sqrt{\left[\left(\beta_{xxx} + \beta_{xxy} + \beta_{xyy}\right)^2 + \left(\beta_{yyy} + \beta_{xxz} + \beta_{yyz}\right)^2 + \left(\beta_{xzz} + \beta_{yzz} + \beta_{zzz}\right)^2\right]}$$

The values of the polarizabilities (α) and first hyperpolarizability (β_{tot}) of the Gaussian 09 output are reported in atomic units (a.u.). All the calculated values then have been converted into electrostatic units (esu). (For α: 1a.u. = 0.1482×10^{-24} esu; For β: 1a.u. = 8.639×10^{-33} esu).The mean polarizability (α_o) and total polarizability ($\Delta\alpha$) of our title molecule are   -68.4876 au or -101.499×10^{-24} esu and 20.38369 a.u or 30.2086×10^{-24} esu respectively. The total molecular dipole moment and first order hyperpolarizability are 3.3688 Debye and 427.987×10^{-30} esu , respectively and are depicted in Table IV.Total dipole moment of title molecule is approximately 2.453 times greater than that of urea and first order hyperpolarizability is very much greater than that

639

International Journal for Research in Applied Science & Engineering Technology (IJRASET)

of urea (μ and β of urea are 1.3732 Debye and 0.3728×10^{-30} esu) obtained by B3LYP/6-31+ G(d,p) method. This result indicates the nonlinearity of the title molecule.

TABLE IV

THE CALCULATED ELECTRIC DIPOLE MOMENT, POLARIZABILITY AND FIRST ORDER HYPERPOLARIZABILITY OF 1C4NB

Dipole moment, μ (Debye)		Polarizability α			First order hyperpolarizability β		
Parameter	Value	Parameter	a.u.	esu(×10^{-24})	Parameter	a.u.	esu (×10^{-33})
μ_x	3.3688	α_{xx}	-81.605	-120.939	β_{xxx}	49.2603	425.56
μ_y	0.0002	α_{xy}	-0.0001	-0.00015	β_{xxy}	0.0024	0.0273
μ_z	0.0002	α_{yy}	-58.855	-87.2231	β_{xyy}	0.0008	0.006911
μ_{total}	3.3688	α_{xz}	0.0004	-0.00059	β_{yyy}	8.5387	73.766
		α_{yz}	-65.002	-96.333	β_{xxz}	-0.0005	-0.00432
		α_{zz}	0.0008	0.001186	β_{xyz}	0.0002	0.0017278
		α_o	-68.4876	-101.499	β_{yyz}	-8.2577	-71.34
		$\Delta\alpha$	20.38369	30.2086	β_{xzz}	0.0001	0.000864
					β_{yzz}	0.0026	0.0246
					β_{zzz}	-0.0003	-0.00259
					β	49.5466	428.0401
first order hyperpolarizability				β_{tot}= (427.987x10^{-30} esu)			

D. Molecular Electrostatic Potential

The molecular electrostatic potential is the potential that a unit positive charge would experience at any point surrounding the molecule due to the electron density distribution in the molecule. The electrostatic potential generated in space by charge distribution is helpful to understand the electrophilic and nucleophilic regions in the title molecule. Electrostatic potential maps, also known as electrostatic potential energy maps, or molecular electrical potential surfaces, illustrate the charge distributions of molecules three dimensionally. Knowledge of the charge distributions can be used to determine how molecules interact with one another. Molecular electrostatic potential (MEP) mapping is very useful in the investigation of the molecular structure with its physiochemical property relationships [33-36].In the electrostatic potential map, the semispherical blue shapes that emerge from the edges of the above electrostatic potential map are hydrogen atoms. The molecular electrostatic potential (MEP) at a point r in the space around a molecule (in atomic units) can be expressed as

$$V(r) = \sum_A \frac{Z_A}{|\vec{R}_{A} - \vec{r}|} - \int \frac{\rho(\vec{r}')}{|\vec{r}' - \vec{r}|}\vec{d}r'$$

Where Z$_A$ is the charge of nucleus A located at R$_A$, $\rho(\vec{r}')$ is the electronic density function of the molecule, and $\vec{r}'$ is the dummy integration variable

The first and second term represent the contributions to the potential due to nuclei and electron respectively. V(r) is the net resultant electrostatic effect produced at the point r by both the electrons and nuclei of the molecule. The molecular electrostatic potential surface MESP which is a 3D plot of electrostatic potential mapped onto the iso electron density surface simultaneously displays molecular shape, size and electrostatic potential values.The Electrostatic potential surface of 1C4NB is shown in Figure 4

International Journal for Research in Applied Science & Engineering Technology (IJRASET)
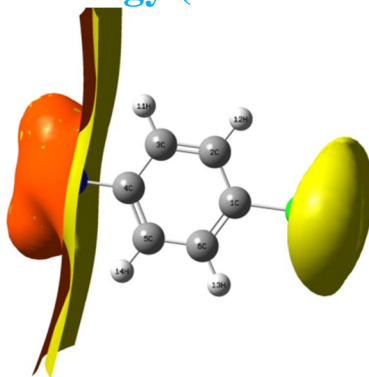

Fig.4 :The Electrostatic potential surface of 1C4NB

Total electron density iso surface mapped with molecular electrostatic potential of 1-chloro-4-nitrobenzene with different views like a) transparent view b) solid view and c) mesh view are shown in Figure 5
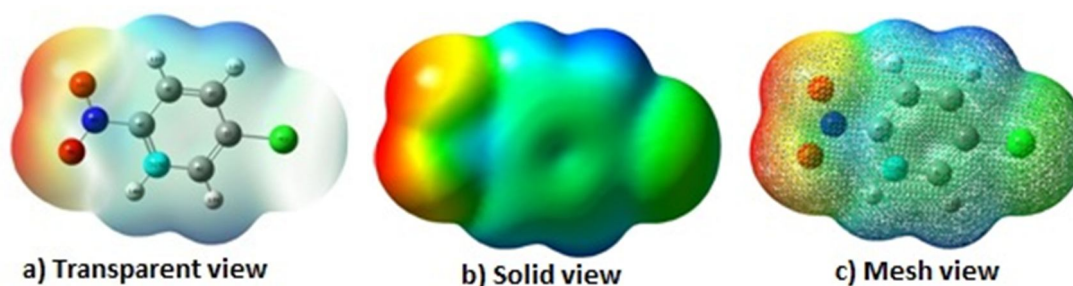

a) Transparent view   b) Solid view   c) Mesh view

Fig 5. Total electron density isosurface mapped with molecular electrostatic potential of 1-chloro-4-nitrobenzene

The colour scheme for the MSEP surface is red - electron rich or partially negative charge; blue - electron deficient or partially positive charge; light blue-slightly electron deficient region; yellow–slightly electron rich region, respectively. Areas of low potential, red, are characterised by an abundance of electrons. Areas of high potential, blue, are characterised by a relative absence of electrons. That is negative potential sites are on the electronegative atoms like nitrogen and oxygen while the positive potential sites around the hydrogen and carbon atoms. Green area covers parts of the molecule where electrostatic potentials are nearly equal to zero   (C-C bond). This is a region of zero potential enveloping the π systems of aromatic ring leaving a more electrophilic region in the plane of hydrogen atom.Nitrogen has a higher electronegativity value would consequently have a higher electron density around them. Thus the spherical region that corresponds to nitrogen atom would have a red portion on it. The MESP of 1C4NB clearly indicates the electron rich centres of nitrogen, oxygen and the areas covering the C4 atom. The contour map of electrostatic potential of 1C4NB has been constructed by the DFT method and is shown in Figure 6. Also confirms the different negative and positive potential sites of the molecule in accordance with the total electron density surface.
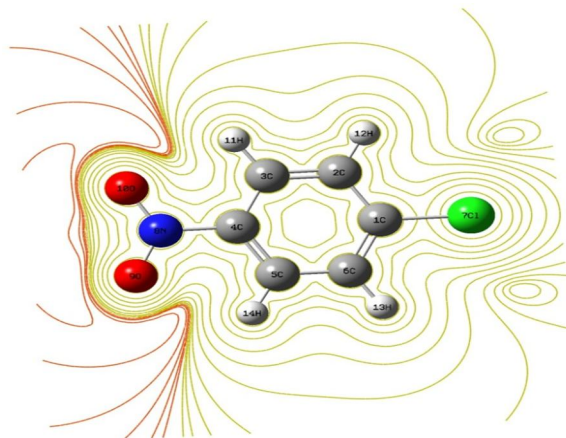

Fig.6. Contour map of molecular electrostatic potential surface of 1-chloro-4-nitrobenzene

641

International Journal for Research in Applied Science & Engineering Technology (IJRASET)

E.   HOMO - LUMO Analysis

When we are dealing with interacting molecular orbitals, the two that interact are generally The Highest energy Occupied Molecular Orbital (HOMO) of one molecule, The Lowest energy Unoccupied Molecular Orbital (LUMO) of the other molecule. These orbitals are the pair that lie closest in energy of any pair of orbitals in the two molecules, which allows them to interact most strongly. These orbitals are sometimes called the frontier orbitals, because they lie at the outermost boundaries of the electrons of the molecules. The energy gap between the HOMOs and LUMOs called as energy gap. It is a critical parameter in determining molecular electrical transport properties because it is a measure of electron conductivity [37].

The HOMO energy characterizes the ability of electron giving, the LUMO characterizes the ability of electron accepting, and the gap between HOMO and LUMO characterizes the molecular chemical stability [38]. Surfaces for the frontier orbital's were drawn to understand the bonding scheme of present compound. The features of these Molecular Orbitals can be seen in Figure 7.

E_{HOMO}= -7.86825 e V ΔE = - 4.75561 e E_{LUMO}= -3.11263 eV
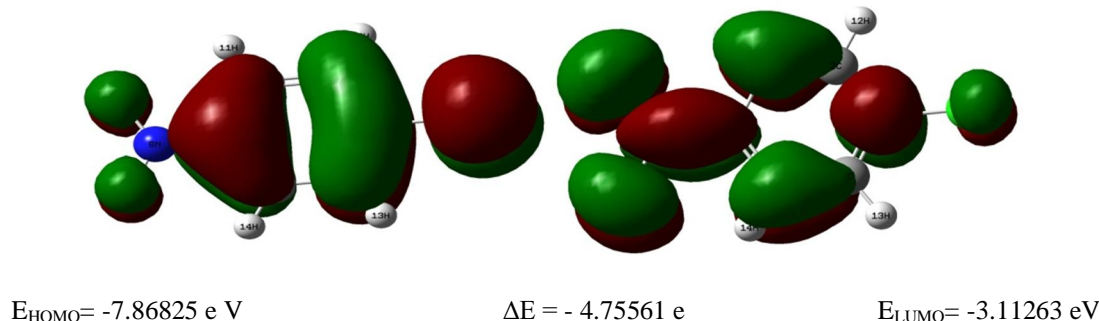
Fig. 7. HOMO LUMO plot of 1C4NB

This electronic absorption corresponds to the transition from the ground state to the first excited state and is mainly described by one electron excitation from HOMO to LUMO. While the energy of the HOMO is directly related to the ionization potential, LUMO energy is directly related to the electron affinity.

There are lots of applications available for the use of HOMO and LUMO energy gap as a quantum chemical descriptor. It establishes correlation in various chemical and bio-chemical systems [39]. The HOMO–LUMO energy gap is an important value for stability index. A large HOMO–LUMO gap implies high stability for the molecule in the sense of its lower reactivity in chemical reactions [40]. According to B3LYP/6-311G+(d,p) calculation, E_{HOMO} , E_{LUMO} and the energy band gap (translation from HOMO to LUMO) of the title molecule in electron Volt are presented in Table V

Table V
HOMO LUMO ENERGIES AND ENERGY GAP OF 1C4NB

Energies	values
E_{HOMO} (eV)	7.868246
E_{LUMO} (eV)	3.112632
E_{HOMO} - E_{LUMO} gap (eV)	-4.755614

F.   Global reactivity descriptors: Electronegativity, hardness, softness and electrophilicity index of the molecule

The electronegativity is based on the fact that the formations of chemical compounds involve electrical forces. Metals and non-metals were seen to possess opposite appetites for the electrical charges. Electronegativity is the tendency of a species to attract electrons. Parr and Yang have given a sketch of attempts to quantify the idea [41]. The hardness of a species (atom, ion, or molecule) is a qualitative indication of how polarizable it is, that is how much its electron cloud is distorted in an electric field. In this sense the terms hard, and its opposite soft, were evidently suggested by D. H. Busch [42] by analogy with the conventional use of these words to denote resistance to deformation by mechanical force. The hardness and softness concept have been extensively used to interpret reactivity.[43] By using HOMO and LUMO energy values for a molecule, the global chemical reactivity descriptors of molecules such as hardness (η), chemical potential (μ), softness (S), electronegativity (χ) and electrophilicity index (ω) can be measured by using Koopman's theorem for closed-shell molecules.

The electronegativity of the molecule given by the equation

$$\chi = \frac{1}{2}(I + A)$$

The hardness of the molecule (η) can be expressed as

$$\eta = \frac{1}{2}(I - A)$$

International Journal for Research in Applied Science & Engineering Technology (IJRASET)

The chemical potential of the molecule is the negative of Hardness

$$\mu = -\tfrac{1}{2}(I - A)$$

The softness of the molecule is the reciprocal of hardness

$$S = 1/\eta$$

The electrophilicity index of the molecule is

$$\omega = \tfrac{1}{2}(\mu^2 S)$$

where $I = -E_{HOMO}$ called Ionisation Potential and $A = -E_{LUMO}$ called electron affinity. The ionization potential I and an electron affinity A of 1C4NB molecule 1C4NB calculated by B3LYP/ 6-311+G(d,p) method is 7.868246 eV and 3.112632eV respectively.

TABLE VI.
ENERGY VALUES OF 1C4NB BY B3LYP/6 311+G(D,P) METHOD

Quantities	values
Hardness [η]	2.377807
Chemical Potential [μ]	-5.490439
Electronegativety [χ]	5.490439
Electropilicity index [ω]	6.338807
Softness [σ]	0.420555

The computed values of the Chemical Hardness is 2.377807, Softness is 0.420555, Chemical potential is -5.490439, Electro negativity is 5.490439 and Electrophilicity index is 5.490439 for our molecule 1C4NB as shown in Table VI . Considering the chemical hardness, large HOMO-LUMO gap represent a hard molecule and small HOMO-LUMO gap represent a soft molecule. From the Table 9, it is clear that the molecule under investigation is very hard since it has a large HOMO-LUMO gap and also having a very small value for softness.

G. Mullikkan charge population analysis

Atomic charges has been used to describe the process of electronegativety equalization and charge transfer in chemical reactions [44,45].Mullikan atomic charge calculation has an important role in the application of quantum chemical calculation to molecular system because atomic charges affect dipole moment ,molecular polarizability, electronic structure and a lot of properties of electronic systems. The Mullikan atomic charges are calculated at B3LYP/6-311+G (d,p) level by determining the electron population of each atom as defined by the basis function and collected in Table VII.

TABLE VII : MULLIKAN ATOMIC CHARGE ON INDIVIDUAL ATOM OF 1C4NB

Atoms	Mullikkan Atomic Charges
C1	1.032504
C2	-0.81873
C3	0.004448
C4	-0.21434
C5	0.004373
C6	-0.8187
Cl7	0.372651
N8	-0.19891
O9	-0.01641
O10	-0.01639
H11	0.171644
H12	0.163106
H13	0.163115
H14	0.171646

A Graph of Mullikan atomic charge on individual atom of 1C4NB was drawn and given in Figure 8. it is worthy to mention that C1,C3 and C5 atoms of the title molecule exhibit positive charge where as C2,C4 and C6 atoms exhibit negative charges. Each

643

International Journal for Research in Applied Science & Engineering Technology (IJRASET)

oxygen atom has nearly equal negative charge 0.01639 for O10 and 0.01641 for O9 atom in the NH_2 group. The Chlorine atom Cl7 has positive charge about 0.372651. All hydrogen atoms exhibit positive charge which are nearly equal. The carbon atom C1 has the highest positive charge (1.032504) when compared with all other carbon atoms in the benzene ring. The presence of large negative charge on nitrogen (N8) and two oxygen (O9 & O10) atoms and net positive charges on hydrogen atom suggest that the formation of intermolecular interaction in solid forms. The Mullikan atomic charges at each atomic site of the 1C4NB was displayed in Figure 1
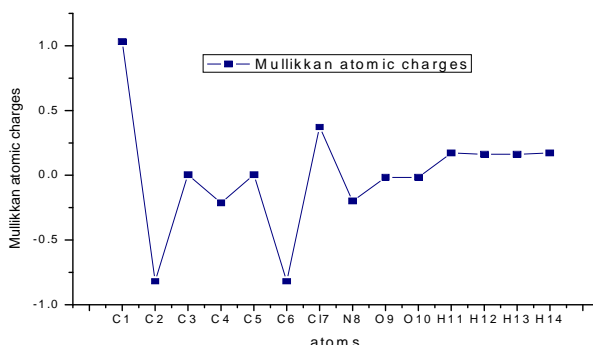

Fig.8 Graph of Mullikan atomic charge on individual atom of 1C4NB

H. UV-Vis spectral analysis

UV-Visible spectroscopy (radiations with wavelengths between 10 and 1000 nm) offers information about the transition of the most external electrons of the atoms. Since atoms or molecules absorb UV-Visible radiation at different wavelength, spectroscopy is often for the identification of substances through the spectrum emitted from or absorbed by them. The Time Dependant Density Functional Density (TD-DFT) Calculation has been performed for 1C4NB on the basis of fully optimized ground state structure to investigate the electronic absorption properties.
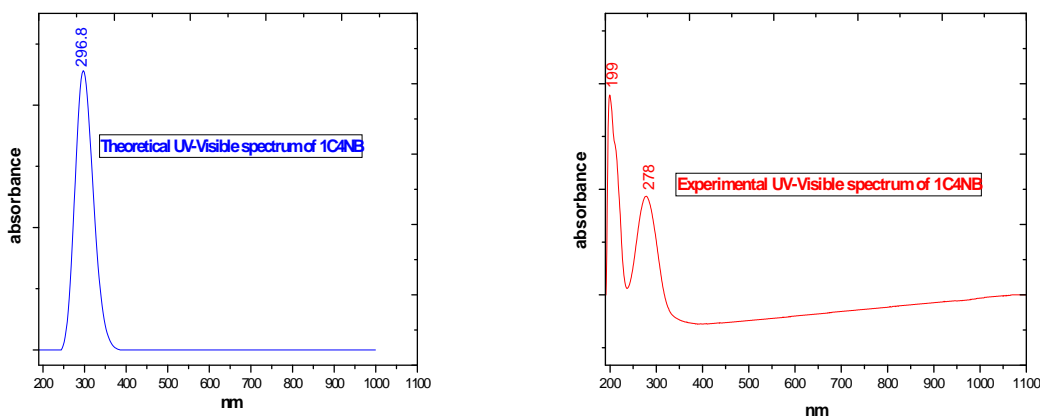

Fig.9. The UV-Visible spectrum of 1C4NB

TD-DFT is able to detect accurate absorption wavelengths at a relatively small computing time which correspond to vertical electronic transitions computed on the ground state geometry, especially in the study of solvent effect [46–48]; Thus TD-DFT method is used with B3LYP function and 6-311G+(d,p) basis set for vertical excitation energy of electronic spectra. The calculated visible absorption maxima of wave length λ_{max} which are a function of the electron availability have been reported in Table VIII. The excitation energies, wave length and oscillator strengths for the title molecule at the optimized geometry in the ground state were obtained in the frame work of TD-DFT calculations with the B3LYP/6-31G(d,p) method. The Theoretical and experimental UV-Visible spectrum is shown in Figure.9. The computed UV spectra predicts one intense electronic transition at 298.84 nm with an oscillator strength f = 0.4094 a.u where as the experimental spectrum gives two intense electronic transitions at 199 nm and 278 nm. The theoretical and experimental values may be slightly shifted by solvent effects. The role of substituent and role of the

International Journal for Research in Applied Science & Engineering Technology (IJRASET)

solvent influence the UV-Visible spectrum. This band may be due to electronic transition of the benzene ring to chlorine atom (transition of π-π*). Both the (HOMO) and (LUMO) are the main orbitals that take part in chemical stability [49]. Calculations of molecular orbital geometry show that the visible absorption maxima of title molecule correspond to the electron transition between frontier orbitals such as transition from HOMO to LUMO. The λ_{max} is a function of substitution. The stronger the donor character of the substitution, the more electrons pushed into the molecule, the larger λ_{max}.

TABLE VIII.
THEORETICAL ELECTRONIC ABSORPTION SPECTRA VALUES OF 1C4NB

Excited State	Energy (eV)	Wavelength λ (nm)	Oscillator strengths (f)
1	1.9201	645.71	0.0001
2	3.8574	321.42	0.0003
3	4.1194	300.97	0.0005
4	4.1488	298.84	0.4094
5	4.3822	282.93	0.0602
6	4.6456	266.89	0.0001

I. ^{13}C and ^{1}H NMR spectral analysis
NMR or Nuclear Magnetic Resonance spectroscopy is a technique used to determine the unique structure of a compound. It identifies the Carbon-Hydrogen framework of an organic compound. The basic principle behind the NMR technique is that the atomic nucleus is a spinning charged particle, and it generates a magnetic field[50]. Without an external applied magnetic field, the nuclear spins are random and spin in random directions. But, when an external magnetic field is present, the nuclei align themselves either with or against the field of the external magnet.
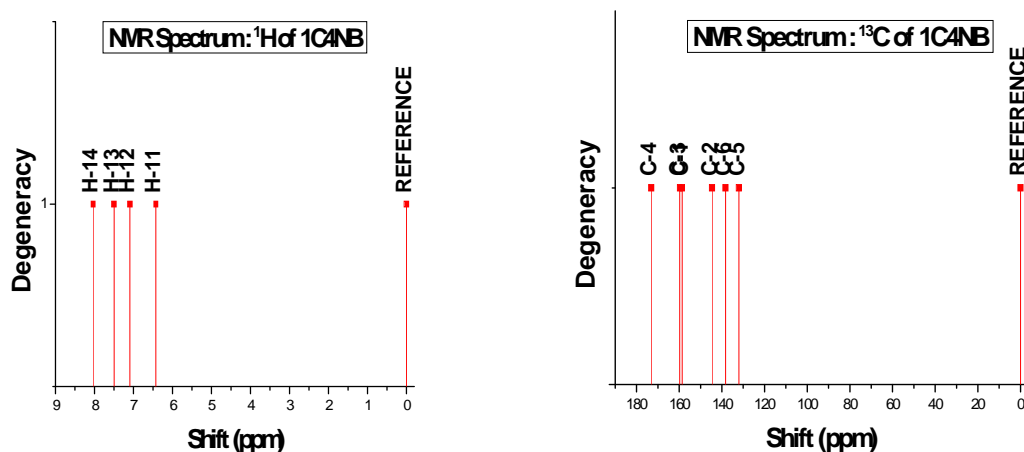

Fig 10. Theoretically calculated NMR Spectrum of ^{1}H and ^{13}C of 1C4NB

Chemical Shift is the measure of how far the signal produced from the proton is from the reference compound signal. TetraMethylSilane (TMS) is usually used as the reference compound because it can easily be removed from the sample by evaporation due to its volatile properties. TMS is at a lower frequency than most other signals because its methyl protons are in a more electron dense environment than most protons are because silicon is less electronegative than carbon (which is a significant component of organic molecules.) The TMS or reference compound is at the zero position on the very left of the spectrum, and as it moves toward the left, the ppm values become larger. Parts per million (ppm) is the unit used to measure chemical shift. Recently, Gauge Invariant Atomic Orbital's (GIAO) Nuclear Magnetic Resonance DFT calculations have become more popular [51] and can successfully predict the chemical shift (in ppm) for small isolated molecules [52-54]. However, the accuracy of NMR theoretical predictions depend on the implemented basis set, and optimized structural parameters. Therefore, structural parameters obtained

645

International Journal for Research in Applied Science & Engineering Technology (IJRASET)

with the hybrid B3LYP functional at the 6-311G+(d,p) level of theory were used to predict ^{1}H and ^{13}C chemical shifts utilizing the recommended GIAO approach [55]. The theoretically computed ^{13}C and ^{1}H NMR spectrum are shown in Figure 10. Relative chemical shifts were estimated by using the corresponding TMS shielding calculated in advance at the same theoretical level as the reference. Aromatic ring carbons give signals in overlapped areas of the spectrum with chemical shift values from 100 to 150 ppm [56,57]. The electro negativity affects the chemical shift as The electron cloud shields the nucleus from the applied magnetic field. The electro negativity is defined as the tendency of an atom to pull electrons toward it.

Therefore, electronegative atoms remove electron density from the proton. This causes the proton to have less electron density, and this leads to less shielding. If the proton has less shielding, it will feel the applied magnetic field more, and this leads to a higher energy and a higher chemical shift. Protons that are closer to the electronegative atom are in a less electron dense environment, which means that their chemical shifts will be larger. It can be seen from table, that due to the influence of electronegative nitrogen atom, the chemical shift values of carbon atoms are significantly changes the shift positions in the range 150 to 180 ppm. Thus, the C4 atom has its chemical shifts at 173.1638 ppm. The chemical shift value of Carbon atom attached with chlorine atom is 158.6214 due to the shielding effect. As the C3 atom is near to nitrogen atom it's chemical shift is at 159.7433. The proton or hydrogen chemical shifts range from 0 ppm to 15 ppm. The chemical shift values of all other Carbon and Hydrogen atoms are reported in TABLE IX.

TABLE IX.
THEORETICAL ISOTROPIC CHEMICAL SHIFT CALCULATED USING DFT B3LYP/6-311 G+(D,P) (WITH RESPECT TO TMS, ALL VALUES IN PPM) FOR 1C4NB

Calculated chemical shift (ppm)	
Atom	**B3LYP/6-311G+(d,p)**
C1	158.6214
C2	144.5815
C3	159.7433
C4	173.1638
C5	132.0128
C6	138.2318
H11	6.425895
H12	7.090481
H13	7.497315
H14	8.033016

J. Thermodynamic analysis

The values of some thermodynamic parameters such as Total thermal energy, heat capacity at constant volume, entropy, zero point vibrational energies, rotational constants are obtained at standard condition for optimized geometry of 1C4NB with B3LYP/6-311 g(d,p) basis set are given in Table X.

TABLE X.
THE CALCULATED THERMODYNAMICAL PROPERTIES OF 1C4NB

Thermodynamical parameters	B3LYP/6-311+G(d,p)	
Total Energy (Thermal) $E_{Thermal}$ [KCal/Mol]	57.558	
Heat Capacity at constant volume,C_V [Cal/Mol-Kelvin]	32.741	
Entropy S [Cal/Mol-Kelvin]	93.849	
Zero-point vibrational energy E_0 [Kcal/Mol]	52.047	
Vibrational Energy, E_{vib} [Kcal/Mol]	55.781	
Rotational constants (GHZ)	A	3.97184
	B	0.56607
	C	0.49546

646

International Journal for Research in Applied Science & Engineering Technology (IJRASET)

The zero point energies, thermal correction to internal energy, enthalpy, Gibbs free energy, entropy as well as the heat capacity for a molecular system were computed from the frequency calculations. The computed thermodynamic parameters are listed in Table XI.

TABLE XI.

THE TEMPERATURE DEPENDENCE OF THERMODYNAMIC PARAMETERS OF 1C4NB

Temperature (Kelvin)	Thermal Energy E [KCal/Mol]	Entropy S (Cal/Mol-Kelvin)	Heat Capacity Cv (Cal/Mol-Kelvin)
100	52.991	68.40	13.48
200	54.812	82.01	23.11
300	57.619	94.06	32.91
400	61.346	105.30	41.32
500	65.82	115.70	47.89
600	70.871	125.26	52.91
700	76.364	134.02	56.79
800	82.202	142.08	59.85
900	88.315	149.51	62.32
1000	94.65	156.39	64.33

On the basis of vibrational analysis, the thermodynamic functions such as heat capacity at constant pressure (Cp), entropy (S) and enthalpy change (ΔH) for title compound were determined and listed in Table 4. The correlation of heat capacity at constant pressure (Cp), entropy (S) thermal energy (E) with temperature were plotted in Fig.11 The entropies, heat capacities, and thermal energies are increasing with temperature [58] ranging from 100 to 1000 K due to the increase in vibrational intensities with temperature. In the case of 1C4NB, all thermodynamic parameters have been increased steadily. As per the second law of thermodynamics in thermo chemical field , these calculations can be used to compute the other thermodynamic energies and helps to estimate the directions of chemical reactions.
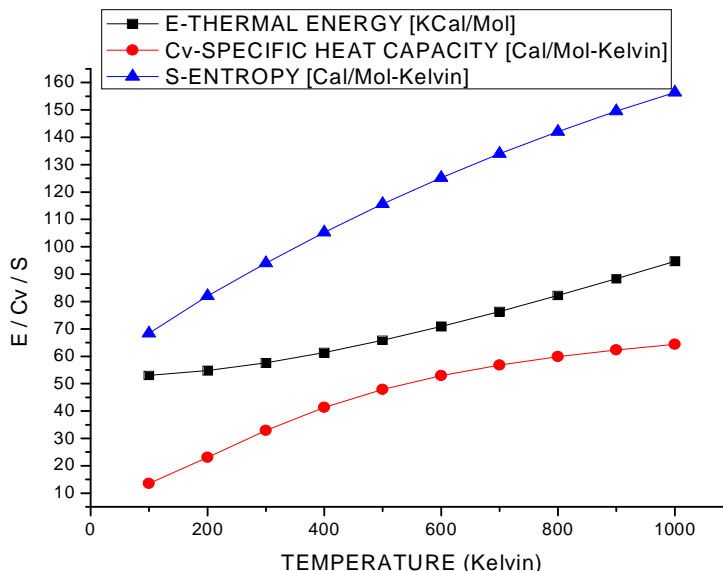

Fig 11. Temperature dependence of thermal energy, heat capacity at constant Volume and Entropy with temperature of 1-chloro-4-nitrobenzene

VI.   CONCLUSION

The fundamental vibrational frequencies and intensities of vibrational bands were calculated using density functional theory (DFT) with the standard B3LYP/6-311+G(d.p) method and frequencies were scaled using various scale factors. Simulation of infrared and Raman spectra utilizing the results of these calculations led to excellent overall agreement with the observed spectra. The ^{1}H and [13]C

647

International Journal for Research in Applied Science & Engineering Technology (IJRASET)

nuclear magnetic resonance chemical shifts of the molecule were also calculated using the GIAO (gauge independent atomic orbital) method. The theoretical and experimental UV–VIS spectra of   title compound were studied. The electronic properties, such as HOMO (Highest Occupied Molecular Orbital) and LUMO (Lowest Unoccupied Molecular Orbital) energies were performed by time-dependent DFT (TD-DFT) approach. The difference in HOMO and LUMO energy supports the interaction of charge transfer within the molecule Information about the size, shape and charge density distribution and site of chemical reactivity of the molecule has been obtained by mapping electron density isosurface with Molecular Electro Static Potential (MESP). The dipole moment , polarizability , first order hyperpolarizability and mullikkan atomic charges of the title molecule were calculated using DFT calculations. In addition Chemical reactivity ,The thermodynamic properties (heat capacity at constant volume, entropy and enthalpy changes) in the temperature ranges from 100 to 1000 K ,Rotational constants, a zero point vibrational energy and SCF energy of 1C4NB were also calculated.

VII.   ACKNOWLEDGEMENT

REFERENCES

[1]   Hazardous Substances Data Bank (HSDB, 1997). National Library of Medicine. Bethesda, MD
[2]   Gerald Booth "Nitro Compounds, Aromatic" in Ullmann's Encyclopedia of Industrial Chemistry, Wiley-VCH: Weinheim, 2005
[3]   M.J. Frisch, G.W. Trucks, H.B. Schlegal, G.E. Scuseria, M.A. Robb, J.R. Cheesman, V.G. Zakrzewski, J.A. Montgomery Jr., R.E. Stratmann, J.C. Burant, S. Dapprich, J.M. Millam, A.D. Daniels, K.N. Kudin, M.C. Strain, O. Farkas, J. Tomasi, V. Barone, M. Cossi, R. Cammi, B. Mennucci, C. Pomkelli, C. Adamo, S. Clifford, J. Ochterski, G.A. Petersson, P.Y. Ayala, Q. cui, K. Morokuma, N. Rega, P. Salvador, J.J. Dannenberg, D.K. Malilck, A.D. Rabuck, K. Raghavachari, J.B. Foresman, J. Cioslowski, J.V. Ortiz, A.G. Baboul, B.B. Stefanov, G. Liu, A. Liashenko, P. Piskorz, I.Komaromi,R.Gomperts, R.L. Martin, D.J. Fox, T.Keith,M.A. Al-Laham, C.Y. Peng, A.Nanayakkara, M. Challa-Combe, P.M.W. Gill, B. Johnson,W. Chen,M.W.Wong, J.L. Andres, C. Gonzalez, M. Head-Gordon, E.S. Replogle, J.A. Pople, Gaussian 98, Revision A 11.4, Gaussian Inc., Pittsburgh, PA, 2002.
[4]   A.D. Becke, J. Chem. Phys. 98 (1993) 5648.
[5]   C. Lee,W. Yang, R.C. Parr, Phys. Rev. B 37 (1998) 785.
[6]   P. Pulay, G. Fogarasi, G. Pongor, J.E. Boggs, A. Vargha, J. Am. Chem. Soc. 105 (1983)7037.
[7]   G. Rauhut, P. Pulay, J. Phys. Chem. 99 (1995) 3093.
[8]   G. Fogarasi, P. Pulay, in: J.R. Durig (Ed.), Vibrational Spectra and Structure, vol. 14, Elsevier, Amsterdam, 1985, p. 125.
[9]   G. Fogarasi, X. Zhou, P.W. Taylor, P. Pulay, J. Am. Chem. Soc. 114 (1992) 8191.
[10]   T. Sundius, J. Mol. Struct. 218 (1990) 321.
[11]   T. Sundius, Vib. Spectrosc. 29 (2002) 89–95; (b) Molvib (V 7.0): Calculation of Harmonic Force   Fields and Vibrational Modes of Molecules, QCPE Program No. 807 (2002).
[12]   F.A. Cotton, Chemical Applications of Group Theory, Wiley Interscience, New York, 1971.
[13]   A. Frisch, A.B. Nielson, A.J. Holder,GaussviewUsers Manual, Gaussian Inc., Pittsburgh, PA, 2000.
[14]   G. Keresztury, S. Holly, J. Varga, G. Besenyei, A.V. Wang, J.R. Durig, Spectrochim. Acta 49 A (1993) 2007.
[15]   G. Keresztury, in: J.M. Chalmers, P.R. Griffiths (Eds.), Handbook of Vibrational Spectroscopy, vol. 1, John Wiley and Sons Ltd., 2002, p. 71.
[16]   G. Keresztury, in: J.M. Chalmers, P.R. Griffiths (Eds.), Handbook of Vibrational Spectroscopy, vol. 1, John Wiley and Sons Ltd., 2002, p. 71
[17]   A. Teimouri, A.N. Chermahini, K. Taban, H.A. Dabbagh, Spectrochim. Acta A 72 (2009) 369–377
[18]   G. Keresztury, Raman spectroscopy: theory, in: J.M. Chalmers, P.R. Griffiths(Eds.), Handbook of Vibrational Spectroscopy, vol. 1,   John Wiley &Sons Ltd., 2002, p. 71
[19]   W. Zierkiewiez, D. Michalska, Th. Zeegers-Huyskens, J. Phys. Chem. 104A(2000) 11685]. Mooney et al.
[20]   E.F. Mooney, Spectrochim. Acta 20 (1964) 1021.
[21]   E.F. Mooney, Spectrochim. Acta 19 (1963) 877.
[22]   V.J. Eatch, D. Steel, J. Mol. Spectrosc. 48 (1973) 446–449.
[23]   R.A.R. Pearce, D. Steel, K.J. Radcliffe, J. Mol. Struct. 15 (1973) 409–414.–54
[24]   D.N. Sathyanarayana, Vibrational Spectroscopy – Theory and Applications, second ed., New Age International (P) Limited Publishers, New Delhi, 2004.
[25]   E.K. Meislich, H. Meislich, J. Sharefkin, 3000 Solved Problems in Organic Chemistry, vol. 2, McGraw-Hill, New York, 1993.
[26]   P.M. Champion, A.C. Albrecht, Annu. Rec. Phys. Chem. 33 (1983) 353.
[27]   R.P. Rava, T.G.J. Spiro, Phys. Chem. 89 (1985) 2089.
[28]   A.J. Abkowicz-Bienko, D.C. Bienko, Z. Latajka, J. Mol. Struct. 552 (2000) 165–175.
[29]   S. George, Infrared and Raman Characteristic Group Frequencies-Tables and Charts, third ed., Wiley, New York, 2001.
[30]   A. Kovacs, G. Keresztury, V. Izvekow, Chem. Phys. 253 (2000) 193.
[31]   C. Andraud, T. Brotin, C. Garcia, F. Pelle, P. Goldner, B. Bigot, A. Collet, J. Am. Chem. Soc. 116 (1994) 2094–2101
[32]   D.A. Kleinman, Phys. Rev. 126 (1977) 1962–1979
[33]   I. Fleming, Frontier Orbitals and Organic Chemical Reactions, John Wiley and Sons, New York, pp. 5–27, 1976.
[34]   J.S. Murray, K. Sen, Molecular Electrostatic Potentials, Concepts and Applications, Elsevier, Amsterdam, 1996.
[35]   J.M. Seminario, Recent Developments and Applications of Modern Density Functional Theory, Vol.4, Elsevier, pp 800–806, 1996.
[36]   T. Yesilkaynak, G. Binzet, F. Mehmet Emen, U. Florke, N. Kulcu, H. Arslan, Eur. J. Chem. 1 (2010) 1
[37]   D.F.V. Lewis, C. Loannides, D.V. Parke, Xenobiotica 24 (1994) 401–408.

International Journal for Research in Applied Science & Engineering Technology (IJRASET)

[38]   Mehmet Karabacak, Mehmet Cinar, Mustafa Kurt, Spectrochim. Acta Part A Mol. Biomol. Spectrosc. 74 (2009) 1197–1203.

[39]   Z. Zhou, R.G. Parr, J. Am. Chem. Soc. 112 (1990) 5720–5724

[40]   R. Ditchfield, Mol. Phys. 27 (1974) 789–807.

[41]   R. G. Parr and W. Yang, "Density-Functional Theory of Atoms and Molecules," OxfordUniversity Press, New York, 1989 p 91-95

[42]   R. G. Pearson, J. Am. Chem. Soc., 1963, 85, 3533. (b) R. G. Pearson, Science, 1963,151, 172

[43]   K. Govindarasu, E. Kavitha, Molecular structure, vibrational spectra, NBO, UV and first order hyperpolarizability, analysis of 4-Chloro-dl-phenylalanine by density functional theory, Spectrochimica Acta Part A: Molecular and Biomolecular Spectroscopy, 133 (2014) 799-810

[44]   S. Fliszar, Charge Distributions and Chemical Effects, Springer, New York, 1983.

[45]   E. Smith, J. Am. Chem. Soc. 113 (1991) 6029–6037.

[46]   D. Jacquemin, J. Preat, E.A. Perpete, Chem. Phys. Lett. 40 (2005) 254-259.

[47]   D. Jacquemin, J. Preat, M. Charlot, V. Wathelet, J.M. Andre, E.A. Perpete, J. Chem. Phys. 121 (2004) 1736-1744.

[48]   M. Cossi, V. Barone, J. Chem. Phys. 115 (2001) 4708-4717.

[49]   S. Gunasekaran, R.A. Balaji, S. Kumeresan, G. Anand, S. Srinivasan, Can. J. Anal. Sci. Spectrosc. 53 (2008) 149-161.

[50]   S.Seshadri, Rasheed.M.P ,R.Sangeetha ,IOSR-J. Appl.Chem 8(2015) 87-100

[51]   A.D. Becke, Phys. Rev. 38A (1988) 3098–3100.

[52]   V.G. Malkin, O.L. Malkina, M.E. Casida, D.R. Salahub, J. Am. Chem. Soc. 116 (1994) 5898–5908.

[53]   D.B. Chesnut, C.G. Phung, J. Chem. Phys. 91 (1989) 6238–6245.

[54]   T. Kupka, M. Kolaski, G. Pasterna, K. Ruud, J. Mol. Struct. THEOCHEM 467 (1999) 63–78.

[55]   H.O. Kalinowski, S. Berger, S. Braun, Carbon-13 NMR Spectroscopy, John Wiley&Sons, Chichester, 1988.

[56]   K. Pihlaja, E. Kleinpeter (Eds.), Carbon-13 Chemical Shifts in Structural and   Sterochemical Analysis, VCH Publishers, Deerfield Beach, 1994.

[57]   D. Arul Dhas, I. Hubert Joe, S.D.D. Roy, T.H. Freeda, Spectrochim. Acta 77 (2010)   36–44.

[58]   S.Seshadri, Rasheed.M.P ,R.Sangeetha ,Int.J.Scie.Res. Appl.Chem 8(2015) 87-100

INTERNATIONAL JOURNAL
FOR RESEARCH

IN APPLIED SCIENCE & ENGINEERING TECHNOLOGY

Call : 08813907089   (24*7 Support on Whatsapp)